Aggregation Behavior of Fluorooctanols in Hydrocarbon Solvents

Akio Ohta,*,† Ryo Murakami,‡ Akiko Urata,† Tsuyoshi Asakawa,† Shigeyoshi Miyagishi,† and Makoto Aratono‡

Department of Chemistry and Chemical Engineering, Faculty of Engineering, Kanazawa University, Ishikawa 920-8667, Japan, and Department of Chemistry, Faculty of Science, Kyushu University, Fukuoka 812-8581, Japan

Received: April 27, 2003; In Final Form: June 29, 2003

The association behaviors of three 1-octanols (1-octanol: C8OH; 1,1,2,2-tetrahydrotridecafluorooctanol: TFC8OH; and 1,1-dihydropentadecafluorooctanol: DFC8OH) in two hydrocarbon solvents (*n*-hexane and benzene) were examined by vibration spectroscopy from 288.15 to 318.15 K. From the analysis of results with a mass action model, it was found that dimers and tetramers of 1-octanols coexisted with monomers in the *n*-hexane solution. These aggregates were formed by hydrogen bonding between the OH groups of 1-octanols. In the *n*-hexane solutions, an increase in the fluorination number of the 1-octanol molecule enhanced the intermolecular hydrogen bonding between the OH groups, but reduced the amounts of polymeric species. Conversely, in the benzene solution, the NIR experiment suggested that the OH groups of 1-octanols did not interact with other OH groups, but with the benzene molecules instead. It was found from ^{19}F NMR chemical shift measurements that the fluorooctanols in the benzene solution aggregated by interaction between the fluorocarbon chains instead of by hydrogen bonding.

Introduction

It is well-known that the interaction between fluorocarbon and hydrocarbon compounds is very weak in comparison to homomolecular interactions. In an aqueous mixed system of an ionic fluorocarbon surfactant and an ionic hydrocarbon surfactant, therefore, two types of micelles, i.e., fluorocarbon-rich and hydrocarbon-rich micelles, are formed separately.[1−7] Although a nonionic fluorocarbon surfactant mixes with a nonionic hydrocarbon surfactant in the micelles, the miscibility is very poor compared to ideal mixtures.[8] Furthermore, it was reported that an anionic hybrid surfactant, which had both a fluorocarbon and a hydrocarbon chain, formed a unique micelle with an unusually long lifetime.[9] A long-chain fluoro alcohol is often used as a starting material for the synthesis of fluorinated surfactants. It is important to investigate the properties of this starting fluoro alcohol in order to understand the behavior of fluorinated surfactants. Takiue et al. reported that (1) the adsorbed film of long-chain fluoro alcohols at an *n*-hexane/water interface was transformed to the condensed state at a lower concentration and interfacial pressure than the long-chain hydrocarbon alcohol,[10] and that (2) the long-chain fluoro alcohol completely separated from the long-chain hydrocarbon alcohol in the condensed interfacial film.[11−13] However, there are few studies of its bulk properties, owing to its low solubility in the absence of halogenated solvents.

It is well established that alcohol molecules form linear dimers or oligomers and cyclic tetramers in nonpolar or inert solvents through intermolecular hydrogen bonding.[14−22] NIR and IR spectroscopy are powerful methods to investigate hydrogen bonds,[23] thus most studies that have been carried out use them. Since the fluorination of the alkyl chain of alcohols causes both an increase in hydrogen-bonding ability and a decrease in affinity to hydrocarbon solvents, it is very interesting to examine the effect of fluorination on the association behavior of fluoro alcohols. On the other hand, we have shown that oleyl alcohol molecules associate without hydrogen bonding between the hydroxyl groups in benzene solution, due to the strong interaction between the hydroxyl groups and the benzene molecules.[22,24] Taking into account the fluorination effect mentioned above, micelle formation in oil solution,[25] i.e., the association of fluoro alcohols in benzene solution, through interactions between the fluorocarbon chains, is predicted.

In this study, the association behaviors of three 1-octanols (1-octanol: C8OH; 1,1,2,2-tetrahydrotridecafluorooctanol: TFC8OH; and 1,1-dihydropentadecafluorooctanol: DFC8OH) in two hydrocarbon solvents (*n*-hexane and benzene) were investigated by density measurements and vibration spectroscopy at temperatures from 288.15 to 318.15 K, and the effect of the fluorination of octanol on self-association was then examined. It was found that fluorination of the β-position of the alcohol had a significant effect on its bulk properties as well as interfacial property.[26] In addition, we also studied the interactions between fluorocarbon chains of TFC8OH in benzene solution by ^{19}F NMR chemical shift and semiempirical MO calculations. These results were analyzed by a mass action model.

Experimental Section

Materials. 1-Octanol (C8OH) and 1,1,2,2-tetrahydrotridecafluorooctanol (TFC8OH) were purchased from Tokyo Chemical Industry Co., Ltd., and purified by distillation under reduced pressure. 1,1-Dihydropentadecafluorooctanol (DFC8OH) was

* Author to whom correspondence should be addressed at Department of Chemistry and Chemical Engineering, Faculty of Engineering, Kanazawa University, 2-40-20 Kodatsuno, Kanazawa, Ishikawa 920-8667, Japan. E-mail: akio-o@t.kanazawa-u.ac.jp.

† Kanazawa University.

‡ Kyushu University.

10.1021/jp035134o CCC: $25.00
Published on Web 09/16/2003

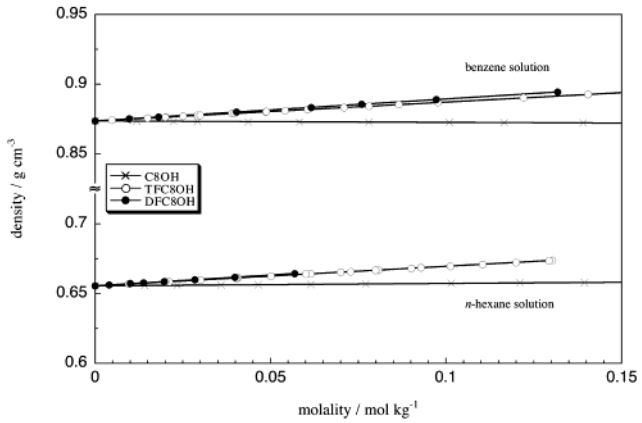

Figure 1. Densities of different 1-octanol solutions vs molality at 298.15 K: C8OH (cross), TFC8OH (open circle), and DFC8OH (full circle).

purchased from Across and used without further purification. Chemical purities were checked by gas−liquid chromatography: these were over 99% for C8OH and TFC8OH, and 98% for DFC8OH. *n*-Hexane (Nacalai Tesque, Inc.) was distilled twice before use. Benzene (Wako Pure Chemical Industries. Ltd., >99.8%) was dehydrated by molecular sieve (0.4 nm, MERCK) before preparing sample solutions. Samples were weighed out, and concentrations were converted into molarities by using density calculations. Measurements were carried out from 288.15 to 318.15 K (at 10 K intervals). Owing to its low solubility, the *n*-hexane solution of DFC8OH was only measured above 298.15 K.

Density. The densities of the sample solutions were measured with an Anton Paar digital density meter (DMA 58), as a function of molality of 1-octanols. The apparatus was calibrated by using the densities of air and water as standards. The temperature precision of the DMA 58 was ±0.01 K.

Absorption Spectroscopy. A Perkin-Elmer lambda 19 UV/VIS/NIR spectrometer was used to obtain the absorption spectra. The absorption of the OH-stretching and its first overtone were measured on the IR (2650−3050 nm) and NIR (1150−1650 nm) regions, respectively. The path lengths used in IR and NIR absorption experiments were 2 mm and 10 mm, respectively. The sample room was maintained to within ±0.1 K.

NMR. ^{19}F NMR chemical shift measurements for the benzene solution of TFC8OH were performed on a JEOL JNM-LA400 NMR spectrometer at 400 MHz and room temperature. C_6D_6 and a C_6D_6 solution of benzotrifluoride were used as a solvent and an external standard (0 ppm), respectively.

Results and Discussion

Figure 1 shows the densities d of several 1-octanol solutions as a function of molality m at 298.15 K. It can be seen that densities increase linearly with increasing molality. Partial molar volume of alcohol v_{alc} was calculated by using the following equations:

$$\varphi = \frac{M_{alc}}{d} - \frac{1000(d - d_0)}{mdd_0} \quad (1)$$

$$v_{alc} = \varphi + m\left(\frac{\partial\varphi}{\partial m}\right)_{T,p} = \left(\frac{\partial m\varphi}{\partial m}\right)_{T,p} \quad (2)$$

Here φ is the apparent molar volume of alcohol, d_0 is the density of pure solvent, and M_{alc} is the molecular weight of alcohol.

TABLE 1: Partial Molar Volumes and the Partial Derivatives of Several Systems

		in *n*-hexane		in benzene		pure state
	T / K	v_{alc}^{∞} / cm^3 mol^{-1}	$\partial v_{alc}/\partial m$ / cm^3 kg mol^{-2}	v_{alc}^{∞} / cm^3 mol^{-1}	$\partial v_{alc}/\partial m$ / cm^3 kg mol^{-2}	v_{alc}^{0} / cm^3 mol^{-1}
C8OH	288.15	157.13	−8.052	160.77	3.846	157.32
	298.15	158.85	−8.219	162.38	3.773	158.63
	308.15	160.72	−8.418	163.67	3.613	159.98
	313.15	162.73	−8.628	165.12	3.462	161.38
TFC8OH	288.15	225.93	−97.13	235.68	−71.59	214.21
	298.15	230.63	−64.79	238.88	−73.68	216.43
	308.15	235.47	−96.03	241.95	−74.47	218.73
	313.15	240.18	−98.93	245.11	−74.41	221.13
DFC8OH	288.15			247.65	−87.60	solid
	298.15	254.31	−116.7	251.59	−88.74	solid
	308.15	257.28	−117.5	254.84	−89.64	solid
	313.15	260.90	−119.1	258.51	−90.69	

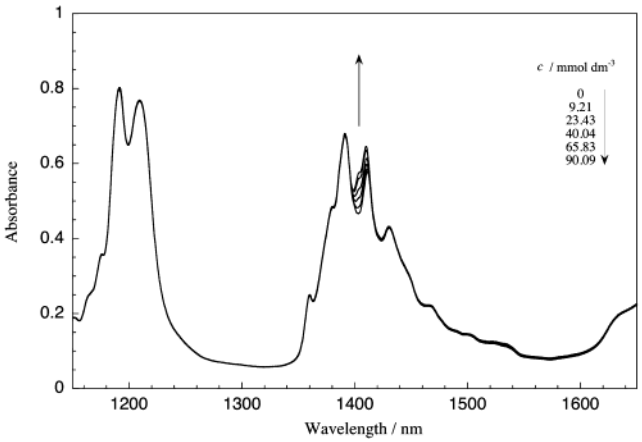

Figure 2. Concentration dependence of NIR spectra of *n*-hexane solutions of C8OH.

The v_{alc} values changed linearly with increasing molality for whole systems. The v_{alc} values at infinite dilution v_{alc}^{∞}, the concentration dependence of partial molar volume $\partial v_{alc}/\partial m$ and the molar volumes of pure alcohol v_{alc}^{0} are shown in Table 1. It was found that the absolute values of $\partial v_{alc}/\partial m$ of fluorooctanols were much larger than those of C8OH. This is attributable to the large gap between v_{alc}^{0} and v_{alc}^{∞} of the fluorooctanol, owing to poor miscibility of the fluorocarbon with the hydrocarbon of solvents. Another interesting point was that the only positive $\partial v_{alc}/\partial m$ values were those of C8OH in the benzene system. This suggests that in this system the interaction between alcohol and solvent molecules is advantageous, while in other systems the interaction between alcohol molecules themselves is governing the volume behavior. Therefore, the self-association of alcohol in solution is contemplated in the latter cases.

Figure 2 shows the concentration dependence of the NIR spectra of the *n*-hexane solution of C8OH at 298.15 K. It can be seen that a relatively sharp absorption band around 1400 nm appears with increasing concentration. This was assigned to the first overtone of the free OH-stretching vibration. As decribed by Iwahashi et al., the NIR spectra of solutions were subtracted from those of pure *n*-hexane by using the peak height of the 1210 nm band, which was assigned to the second overtone of CH asymmetric vibrational stretching of the methylene group.[17,18] From this operation, the absorption spectra of OH-stretching of the alcohol only could be obtained. It is noted that this idea is based on the assumption that the NIR spectrum of CH in the alcohol molecule is identical to that in *n*-hexane. Typical difference spectra obtained for the 1-octanols are shown

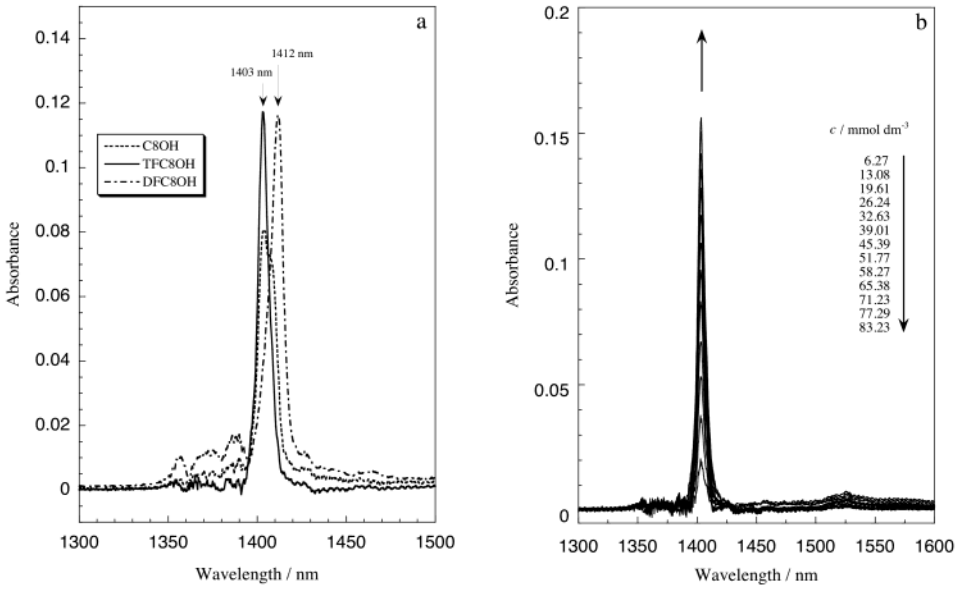

Figure 3. (a) NIR difference spectra of ca. 50 mM solutions of 1-octanols in *n*-hexane at 298.15 K: C8OH (dotted line), TFC8OH (solid line), and DFC8OH (dotted broken line); (b) concentration dependence of NIR difference spectra of *n*-hexane solutions of TFC8OH at 298.15 K.

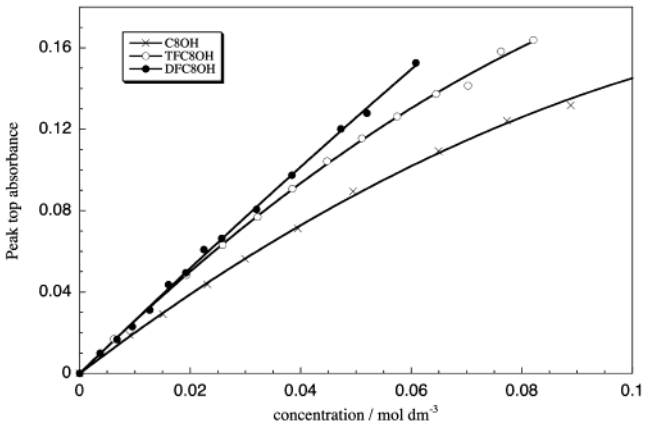

Figure 4. Peak top absorbance of NIR difference spectra of *n*-hexane solutions of 1-octanols vs concentration at 308.15 K: C8OH (cross), TFC8OH (open circle), and DFC8OH (full circle).

in Figure 3: Figure 3a is a comparison among the three 1-octanols at concentrations of about 50 mmol dm^{-3} at 298.15 K, and Figure 3b shows the effect of concentration on the spectra for TC8OH in *n*-hexane at 298.15 K. It was found that only the absorbance of DFC8OH OH-stretching was shifted to a higher wavelength. This suggests that fluorine atoms connected at the β-position of 1-octanol especially enhance the acidity of the OH proton. It was also seen that the absorbance of the free OH group increased with increasing concentration; however, the absorbance of the hydrogen-bonded OH group, which was expected to appear around 1550 nm, was not clear.

The absorbance of the peak top was then plotted against the molarity (*c)* of 1-octanols for the three systems at 308.15 K, an example of which is shown in Figure 4. These plots reflect the concentrations of 1-octanol monomers. We therefore estimated the molar absorption coefficients for 1-octanol monomers by using the slopes of the absorbance vs concentration curves in $c = 0$, where all 1-octanol molecules were in a monomeric state, and then calculated the concentrations of the 1-octanol monomers. Table 2 shows the values of the molar absorption coefficients obtained for 1-octanol monomers. We believe that this evaluation is reliable since they do not rely much on

TABLE 2: Molar Absorption Coefficients of the First Overtone for the Free OH-Stretching Vibration of 1-Octanol Monomers

	$\epsilon_{monomer}$/cm^2 mol^{-1}		
T/K	C8OH	TFC8OH	DFC8OH
288.15	2.13 ± 0.03	2.86 ± 0.06	
298.15	2.10 ± 0.05	2.94 ± 0.03	2.65 ± 0.04
308.15	2.06 ± 0.03	2.92 ± 0.04	2.63 ± 0.05
318.15	2.05 ± 0.02	2.86 ± 0.03	2.60 ± 0.04

temperature. Let us now consider the following consecutive association model:

$$\begin{aligned} &2 \text{ monomer} \rightleftarrows \text{dimer} \\ &\vdots \\ &N \text{ monomer} \rightleftarrows N \text{ mer} \end{aligned} \tag{3}$$

Each association constant K_i is given by

$$K_i = \frac{c_i}{{c_1}^i} \tag{4}$$

where c_i is the molarity of the *i*-mer. Substitution of the mass balance equation

$$c = \sum_{i=1}^{N} i c_i \tag{5}$$

into eq 4 yields the expression

$$c = c_1 + \sum_{i=2}^{N} i K_i {c_1}^i \tag{6}$$

Thus, by fitting the *c* vs c_1 curves to eq 6 with as few parameters as possible, the optimum association constants can be obtained. These results are shown in Figure 5. By employing only dimers and tetramers as polymers, the fitted lines completely matched the experimental data. These results agree with some previous studies on the some oil solutions of alcohol systems.[14,15,19−21] It has also been reported that the dimers and tetramers of

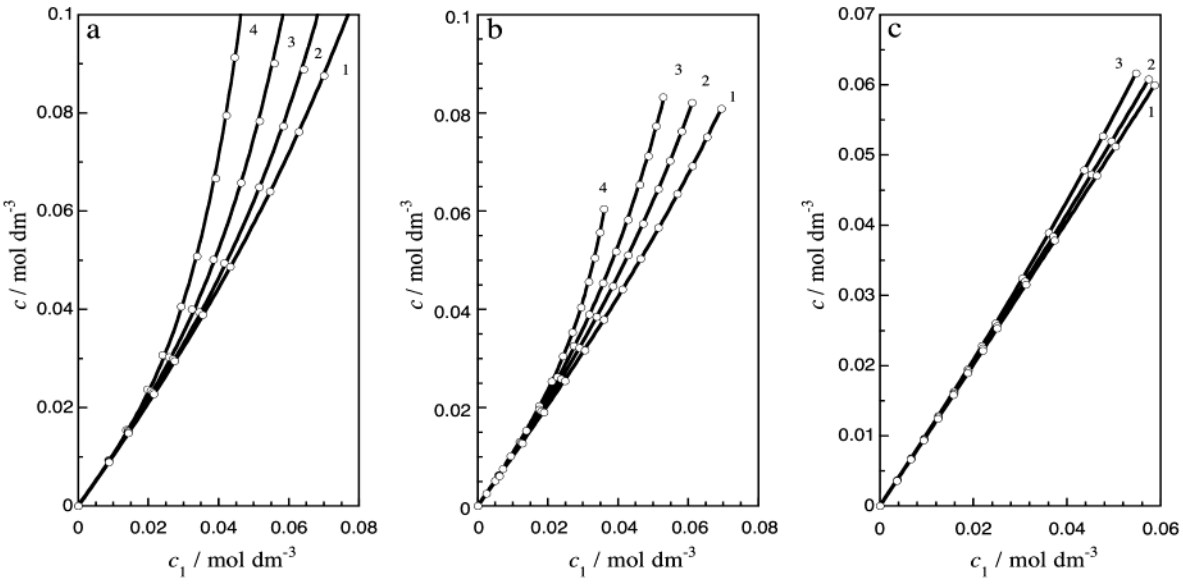

Figure 5. Total concentration of 1-octanol vs concentration of 1-octanol monomers: (a) C8OH, (b) TFC8OH, and (c) DFC8OH; (1) 318.15 K, (2) 308.15 K, (3) 298.15 K, and (4) 288.15 K.

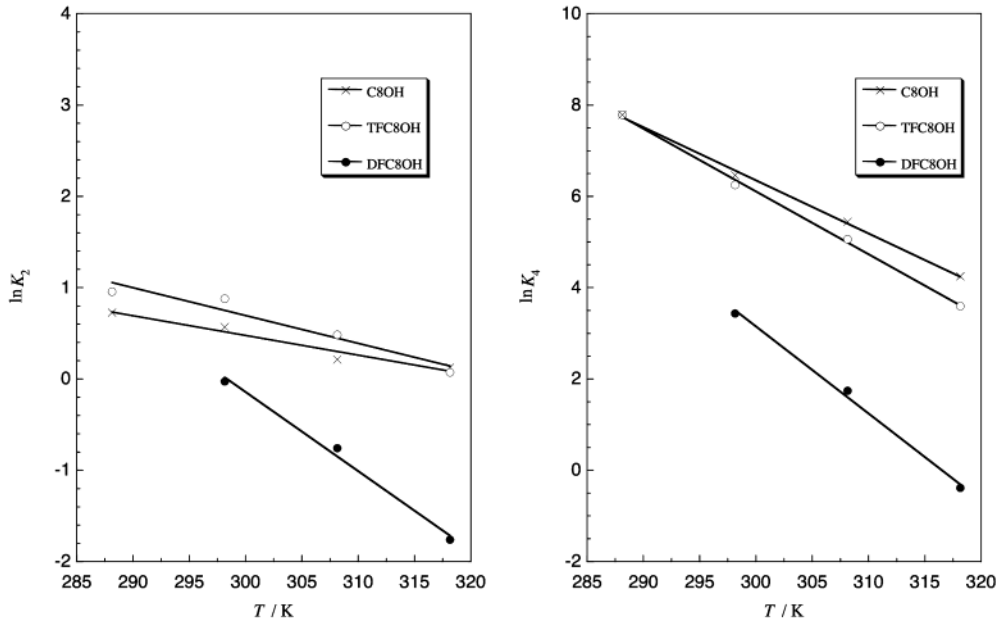

Figure 6. Logarithms of K_2 (left side) and K_4 (right side) vs temperature curves: C8OH (cross), TFC8OH (open circle), and DFC8OH (full circle).

alcohols in nonpolar solutions form linear and cyclic aggregates, respectively.

The logarithms of the association constants obtained (K_2, K_4) were plotted against temperature as shown in Figure 6 for the respective systems: they decreased linearly with rising temperature. The order of K_4 values was DFC8OH ≪ TFC8OH < C8OH, i.e., they decreased with increasing fluorination of the alkyl chain. On the other hand, the K_2 value of TFC8OH was larger than that of C8OH. Further the enthalpies of association $\Delta_i h^*$ were calculated by

$$\Delta_i h^* = \frac{h_i^*}{i} - h_1^* = \frac{RT^2}{i}\left(\frac{\partial \ln K_i}{\partial T}\right)_p \quad (i = 2 \text{ or } 4) \qquad (7)$$

and values at 298.15 K are shown in Table 3. Here, h_i^* is the standard molar enthalpy of the i-mer of 1-octanol molecules. Both $\Delta_2 h^*$ and $\Delta_4 h^*$ values decreased with increasing fluorination number. It is concluded from these results that an increase in fluorination number in 1-octanol molecules enhances the intermolecular hydrogen bonds between the OH groups, but reduces the number of polymeric species. These facts suggest that fluorination of the alkyl chain makes the alkyl chain bulky, therefore favorable orientation of the OH group for association is inhibited. Conversely, in the case of C8OH, it should be taken into account that the entropy loss of the hydrocarbon chain that accompanies association is relatively small because of the flexibility of the hydrocarbon chain. Therefore, association of C8OH can occur despite the low enthalpy of association. However, differences in the thermodynamic properties of association between TFC8OH and DFC8OH were larger than those between TFC8OH and C8OH. It can thus be said that

TABLE 3: Enthalpies of Association of 1-Octanols in *n*-Hexane Solution at 298.15 K

$\Delta_i h^*$/kJ mol^{-1}	C8OH	TFC8OH	DFC8OH
$\Delta_2 h^*$	−8.0	−11.3	−32.0
$\Delta_4 h^*$	− 21.5	−25.4	−35.3

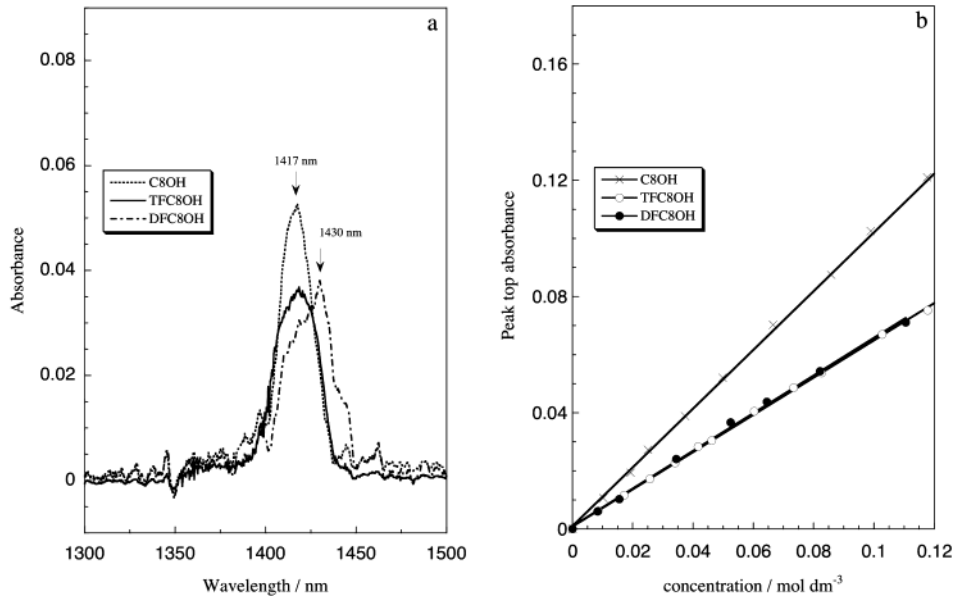

Figure 7. (a) NIR difference spectra of benzene solutions of ca. 50 mM 1-octanols at 298.15 K: C8OH (dotted line), TFC8OH (solid line), and DFC8OH (dotted broken line); (b) peak top absorbance of NIR difference spectra of benzene solutions of 1-octanols vs concentration at 298.15 K: C8OH (cross), TFC8OH (open circle), and DFC8OH (full circle).

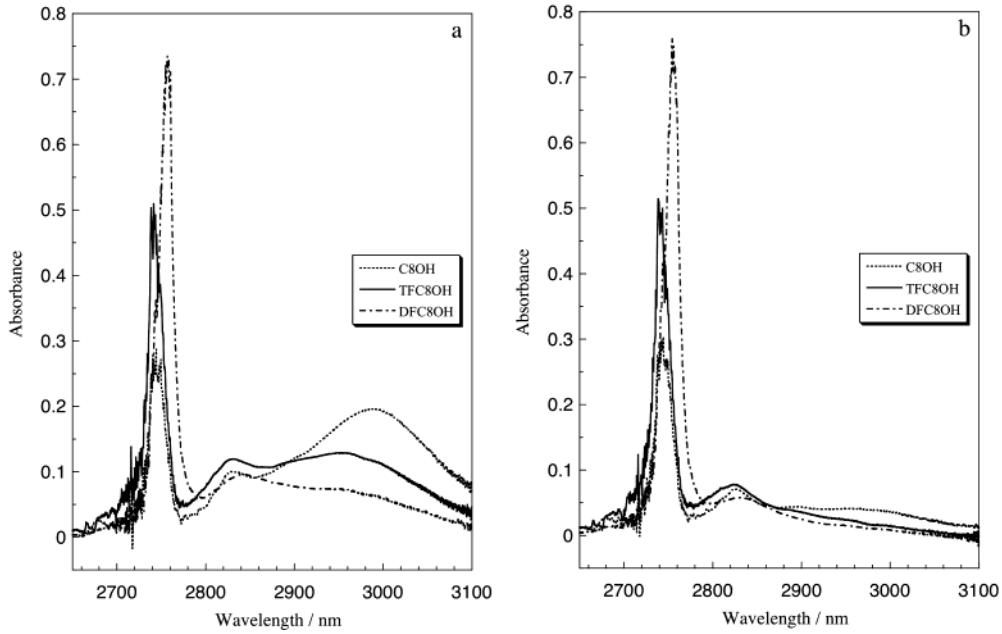

Figure 8. IR difference spectra of ca. 50 mM solutions of 1-octanols in *n*-hexane at 298.15 K: C8OH (dotted line), TFC8OH (solid line), and DFC8OH (dotted broken line); (a) 298.15 K and (b) 318.15 K.

fluorination at the β-position of 1-octanol, rather than the total fluorination number, is the main influence on the solution behavior of a fluorooctanol.

Figure 7a shows the NIR spectra at 298.15 K of the three 1-octanol solutions at about 50 mmol dm^{-3} in benzene. It was found that all the absorbances of the first overtone for OH-stretching of the three 1-octanols were shifted to a wavelength that was about 15 nm higher than that in the *n*-hexane solutions (see Figure 3a). This means that the OH groups interact with benzene molecules. Figure 7b shows the concentration dependence of the absorbance at the peak top at 298.15 K. It can be seen that the absorbance of the OH group increased linearly with increasing concentration over the whole experimental range for the systems. Similar results were obtained at other temperatures (data not shown). It is considered, therefore, that hydrogen-bond formation between alcohol molecules does not occur in benzene solution for either hydrocarbon octanols or fluorocarbon octanols. It follows that the interaction between the OH group of 1-octanol and the benzene molecule may prevent the association of 1-octanol that occurred in the *n*-hexane solutions. Although the hydrogen bonding between 1-octanol molecules was actually superior to the interaction between the OH groups and benzene molecules, the latter exceeded the former in number in this case.

Since the peak of the 1-octanol polymer was not clearly detected in the NIR spectra, we measured the absorbance of the same samples in the IR region (2650−3050 nm). Typical difference spectra are shown in Figures 8 and 9 for *n*-hexane and benzene solutions, respectively. It can be seen that there are three peaks for all three *n*-hexane solution systems (Figure 8).[15,19−23] Judging from the above NIR results, the three peaks might be considered to be the OH-stretching bands of monomer,

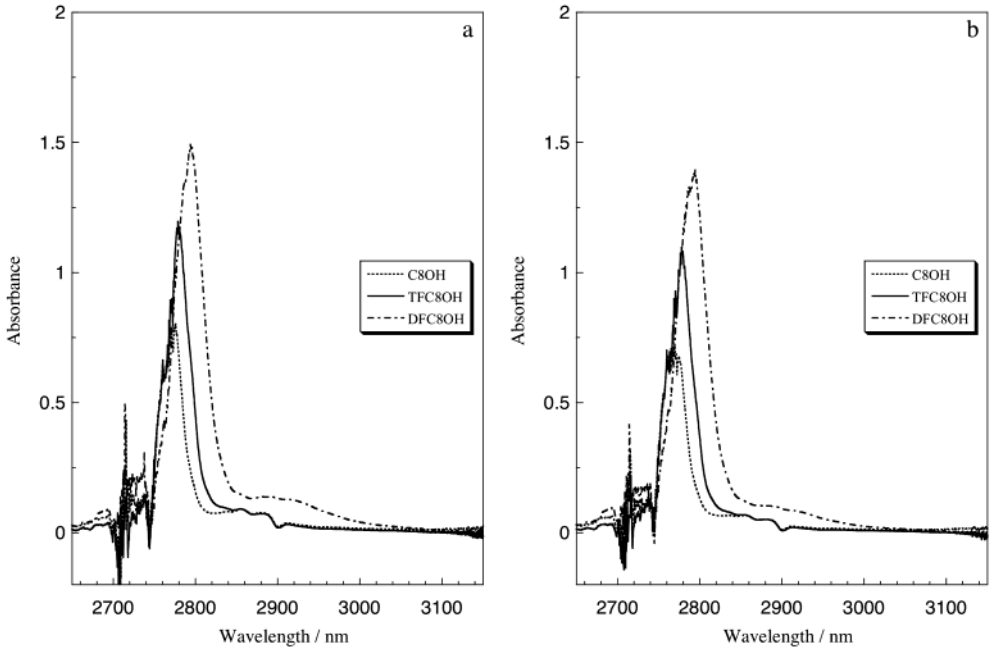

Figure 9. IR difference spectra of ca. 50 mM solutions of 1-octanols in benzene at 298.15 K: C8OH (dotted line), TFC8OH (solid line), and DFC8OH (dotted broken line); (a) 298.15 K and (b) 318.15 K.

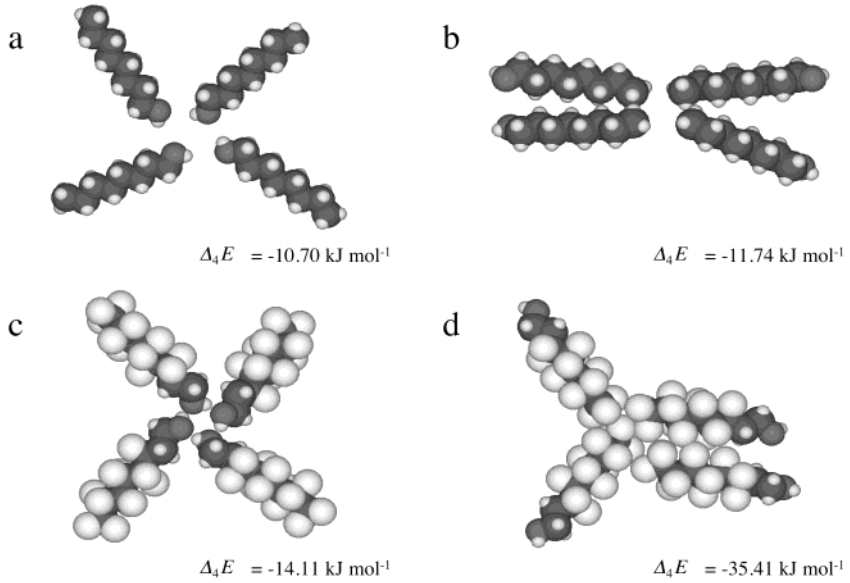

Figure 10. Calculated energies of association and optimized geometries of tetramers of C8OH and TFC8OH: (a) cyclic tetramer of C8OH, (b) micelle-like tetramer of C8OH, (c) cyclic tetramer of TFC8OH, and (d) micelle-like tetramer of TFC8OH.

dimer, and tetramer, respectively, starting from the low wavelength side. The absorbance of polymers increased with increasing concentration, and decreased steeply with rising temperature. Figure 8a shows that the order of the absorbance of tetramers was DFC8OH < TFC8OH < C8OH, while that of the dimers was DFC8OH < C8OH < TFC8OH. Since this matter corresponds to the results of the association constants in Figure 6, the assignment of the IR spectra may be reasonable. On the other hand, there were no significant peaks in the high-wavelength region for the benzene solution systems in Figure 9,[22] although a small shoulder appeared around 2900 nm in the spectra of DFC8OH. The temperature effect was also hardly observed, compared with the *n*-hexane solution systems. This fact strongly supports our claim from the NIR study that hydrogen-bond formation between 1-octanol molecules does not occur in benzene solution. The self-associations of TFC8OH and DFC8OH in benzene solution, however, have been pointed out from the density measurements. We were then obliged to consider that the interaction between fluorocarbon chains was a main driving force for the aggregations.

To examine this model of aggregation formation in detail, we carried out both semiempirical MO calculations of the tetramers of hydrocarbon and fluorocarbon octanols, and the ^{19}F NMR chemical shift measurement of the deuterated benzene solution of TFC8OH. Figure 10 shows the optimized geometries and the energies of association, which are calculated by using MOPAC 2000 with PM3 Hamiltonian in vacuo.[27] Each of the geometries corresponded to the most stable one of eight calculations with different initial configurations. It was seen in the C8OH system that the energy of tetramer gathering of the hydrocarbon chain was almost identical with that of hydrogen bonding between the hydroxyl groups. In the TFC8OH system, however, the former was over twice as large as the latter. This result supports the above association model of the benzene

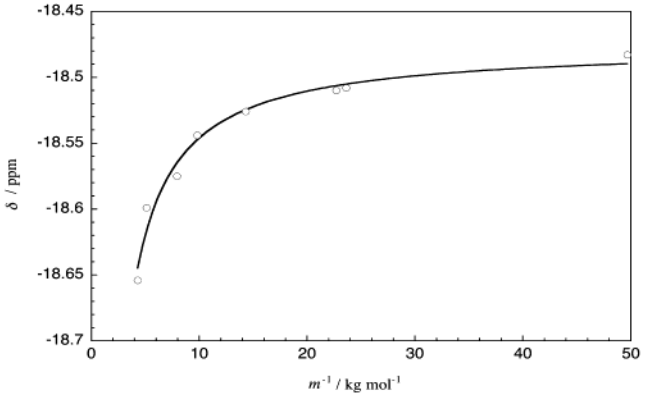

Figure 11. ^{19}F chemical shift of the ω-CF3 peak of TFC8OH in C_6D_6 solution vs reciprocal molality.

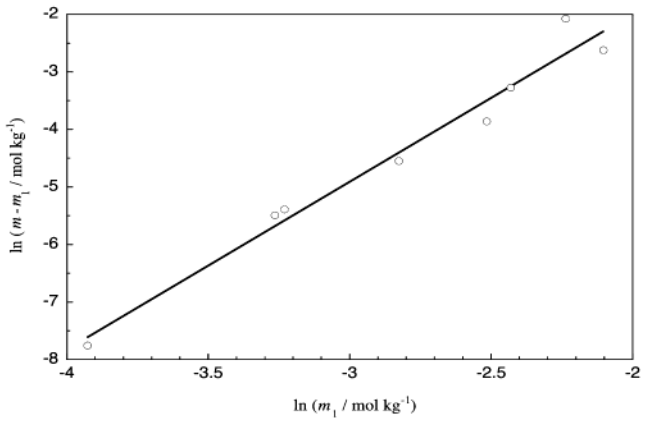

Figure 12. Logarithm of the concentration of aggregate vs logarithm of the concentration of monomer for TFC8OH in C_6D_6 solution.

solution of fluorooctanol. Incidentally, it is well-known that NMR chemical shift is a very sensitive change in atomic environment.[28,29] The ^{19}F NMR chemical shifts of the ω-CF3 group for TFC8OH in C_6D_6 were measured at room temperature as a function of the molality of TFC8OH. The terminal fluorine atoms are the most sensitive to the aggregation. These shifts were plotted against reciprocal concentration $1/m$ as shown in Figure 11. It can be seen that the chemical shifts gradually decreased with increasing molality. Although the variation was not dramatic, this behavior resembled the micellization of fluorocarbon surfactant in water.[28,29] Assuming that this system only contains the monomer and one type of aggregate (*N*-mer), the observed chemical shift can be expressed as an average between the monomer and the *N*-mer.

$$\delta = \frac{m_1}{m}\delta_1 + \frac{Nm_N}{m}\delta_N = \frac{m_1}{m}(\delta_1 - \delta_N) + \delta_N \qquad (8)$$

Here δ_1 and δ_N are the chemical shifts of the monomer and *N*-mer, respectively. Furthermore, by use of a mass action model, we could obtain information about the association number of TFC8OH. From the analogue of eq. 4, the following relation was obtained:

$$\ln Nm_N = \ln(m - m_1) = N \ln m_1 + \ln NK \qquad (9)$$

Here K is the association constant. If we know the values of δ_1 and δ_N, the association number of TFC8OH can be calculated from both eqs 8 and 9. The values of δ_1 and δ_N can be considered as $\lim_{1/m\to\infty}\delta$ and $\lim_{1/m\to 0}\delta$, respectively. Therefore the experimental data in Figure 11 was fitted by the fitting function

$$\delta = \frac{A}{m - B} + \delta_1 \qquad (10)$$

with three parameters A, B, and δ_1. Results obtained are shown in Figure 11 with a solid line, and optimized δ_1 and δ_N were -18.48 and -18.81 ppm, respectively. Thus the left-handed side of eq 9 was plotted against the logarithm of the molality of the monomer in Figure 12. A straight line was obtained, and the association number and constant were then determined by the slope and the intercept, respectively. ($N = 2.9$ and $\ln K = 2.8$)

Conclusions

The association behaviors of three 1-octanols (C8OH, TFC8OH, and DFC8OH) in hydrocarbon solvents (*n*-hexane and benzene) were examined in the temperature range from 288.15 to 318.15 K. From analysis by a mass action model, it was found that dimers and tetramers of 1-octanols coexisted with monomers in the *n*-hexane solution. These aggregates originated from hydrogen bonding between the OH groups of 1-octanols. In the *n*-hexane solution, an increase in the fluorination number of 1-octanol molecules enhanced the intermolecular hydrogen bonding between the OH groups, but reduced the number of polymeric species. In the benzene solutions, however, there was no hydrogen bonding between the OH groups of 1-octanols. From ^{19}F NMR chemical shift measurement, it was found that the TFC8OH molecules gathered in the benzene solution by interactions between the fluorocarbon chains, and the association number was approximately three.

References and Notes

(1) Mukerjee, P.; Yang, A. Y. S. *J. Phys. Chem.* **1976**, *80*, 138.
(2) Shinoda, K.; Nomura, T. *J. Phys. Chem.* **1980**, *84*, 365.
(3) Matsuki, H.; Ikeda, N.; Aratono, M.; Kaneshina, S.; Motomura, K. *J. Colloid Interface Sci.* **1992**, *150*, 331.
(4) Aratono, M.; Ikeguchi, M.; Takiue, T.; Ikeda, N.; Motomura, K. *J. Colloid Interface Sci.* **1995**, *174*, 156.
(5) Asakawa, T.; Hisamatsu, H.; Miyagishi, S. *Langmuir* **1995**, *11*, 478.
(6) Asakawa, T.; Amada, K.; Miyagishi, S. *Langmuir* **1997**, *13*, 4569.
(7) Asakawa, T.; Miyagishi, S. *Langmuir* **1999**, *15*, 3464.
(8) Villeneuve, M.; Nomura, T.; Matsuki, H.; Kaneshina, S.; Aratono, M. *J. Colloid Interface Sci.* **2001**, *234*, 127.
(9) Kondo, Y.; Miyazawa, H.; Sakai, H.; Abe, M.; Yoshino, N. *J. Am. Chem. Soc.* **2002**, *124*, 6516.
(10) Takiue, T.; Yanata, A.; Ikeda, N.; Motomura, K.; Aratono, M. *J Phys. Chem.* **1996**, *100*, 13743.
(11) Takiue, T.; Matsuo, T.; Ikeda, N.; Motomura, K.; Aratono, M. *J Phys. Chem. B* **1998**, *102*, 4906.
(12) Takiue, T.; Matsuo, T.; Ikeda, N.; Motomura, K.; Aratono, M. *J Phys. Chem. B* **1998**, *102*, 5840.
(13) Takiue, T.; Vollhardt, D. *Colloids Surf. A* **2002**, *198−200*, 797.
(14) Bellamy, L. J.; Pase, R. J. *Spectrochimica Acta* **1966**, *22*, 523.
(15) Fletcher, A. N. *J. Phys. Chem.* **1972**, *76*, 2562.
(16) Perz-Casas, S.; Trejo, L. M.; Costas, M. *J. Chem. Soc., Faraday Trans.* **1991**, *87*, 1733.
(17) Iwahashi, M.; Hayashi, Y.; Hachiya, H.; Matsuzawa, H.; Kobayashi, H. *J. Chem. Soc., Faraday Trans.* **1993**, *89*, 707.
(18) Iwahashi, M.; Hachiya, H.; Hayashi, Y.; Matsuzawa, H.; Liu, Y.; Czrnecki, M. A.; Ozaki, Y.; Horiuchi, T.; Suzuki, M. *J. Phys. Chem.* **1995**, *99*, 4155.
(19) Forland, G. M.; Libnau, F. O.; Kvalheim, O. M.; Hoiland, H. *Applied Spectroscopy* **1996**, *50*, 1264.
(20) Forland, G. M.; Libnau, F. O.; Kvalheim, O. M.; Hoiland, H.; Chazy, A. *J Phys. Chem. B* **1997**, *101*, 6960.
(21) Czrnecki, M. A.; Maeda, H.; Ozaki, Y.; Suzuki, M.; Iwahashi, M. *Applied Spectroscopy* **1998**, *52*, 994.
(22) Murakami, R.; Takata, Y.; Ohta, A.; Suzuki, M.; Takiue, T.; Aratono, M. *J Phys. Chem. B* **2002**, *106*, 6548.
(23) Zeegers-Huyskens, T.; Luck, W. A. P. In *Intermolecular Forces*; Huyskens, P. L.; Luck, W. A. P.; Zeegers-Huyskens, T., Eds.; Springer-Verlag: Heidelberg, 1991; Chaps. VI and VII.

(24) Murakami, R.; Takata, Y.; Ohta, A.; Takiue,; Aratono, M. T. *J. Colloid Interface Sci.* submitted.
(25) Fletcher, P. D. I.; Nicholls, R. J.; *Langmuir* **2000**, *16*, 1050.
(26) Takiue, T.; Sugino, K.; Higashi, T.; Toyomasu, T.; Hayami, Y.; Ikeda, N.; Aratono, M. *Langmuir* **2001**, *17*, 8098.
(27) Stewart, J. J. P. *J. Comput. Chem.* **1989**, *10*, 209.
(28) Iijima, H.; Koyama, S.; Fujio, K.; Uzu, Y. *Bull. Chem. Soc. Jpn.* **1999**, *72*, 171.
(29) Bossev, D. P.; Matsumoto, M.; Nakahara, M. *J Phys. Chem. B* **2000**, *104*, 155.